Cavity-Enhanced Parity-Nonconserving Optical Rotation in Metastable Xe and Hg

L. Bougas,[1,2] G. E. Katsoprinakis,[2] W. von Klitzing,[2] J. Sapirstein,[3,*] and T. P. Rakitzis[1,2,†]

[1]*Department of Physics, University of Crete—71003 Heraklion-Crete, Greece*
[2]*Institute of Electronic Structure and Laser, Foundation for Research and Technology-Hellas 71110 Heraklion-Crete, Greece*
[3]*Department of Physics, University of Notre Dame, Notre Dame, Indiana 46556, USA*
(Received 7 December 2011; published 25 May 2012)

We propose the measurement of cavity-enhanced parity-nonconserving (PNC) optical rotation in several transitions of metastable Xe and Hg, including Xe $(^2P^o_{3/2})6s\,^2[3/2]^o_2 \rightarrow (^2P^o_{1/2})6s\,^2[1/2]^o_1$ and Hg $6s6p\,^3P^o_2 \rightarrow 6s6p\,^1P^o_1$, with calculated amplitude ratios of $E^{PNC}_1/M1 = 11 \times 10^{-8}$ and 10×10^{-8}, respectively. We demonstrate the use of a high-finesse bow-tie cavity with counterpropagating beams and a longitudinal magnetic field, which allows the absolute measurement of chiral optical rotation, with a path length enhancement of about 10^4, necessary for PNC measurement from available column densities of 10^{14} cm^{-2} for metastable Xe or Hg. Rapid PNC-signal reversal, allowing robust background subtraction, is achieved by shifting the cavity resonance to an opposite polarization mode or by inverting the magnetic field. The precise measurement of isotope and nuclear-spin dependent E^{PNC}_1 amplitudes provides a sensitive low-energy test of the standard model.

Precise measurements of atomic PNC provide a test of the electroweak part of the standard model at low-energy scale, in contrast to the bulk of such tests that are carried out at the Z-mass energy scale. Several theoretical and experimental constraints have led to atomic PNC [1] being measured in only a handful of systems [2–8]. The most accurate atomic PNC test performed involves the $6s$–$7s$ PNC transition in the only stable isotope of Cs using the Stark-interference technique, for which the E^{PNC}_1 amplitude was measured with a precision of 0.35% [2]. The Cs atomic structure calculations have, with efforts spanning over 20 years [9,10], reached a precision of about 0.25% [11]. Together, experiment and theory constrain new physics beyond the standard model, with the most powerful constraint putting a lower bound of 1.4 TeV/c^2 for extra Z′ bosons [11]. The optical rotation technique has been used to measure E^{PNC}_1 in Tl, Bi, and Pb (see [4–8] and references therein), with Tl being the second-most accurate atomic PNC experiment with a precision of 1% [4]. However, as Tl is essentially a three-valence electron system rather than an alkali, the estimated theoretical accuracy is currently limited to about 3% [12]. Ongoing Stark-interference experiments on Yb have measured the largest E^{PNC}_1 amplitude yet observed [3]. However, theoretical precision in Yb is expected to be poor (currently at 13% [13]); therefore, future experiments are aimed at measuring Yb PNC precisely for several isotopes, as isotope-ratio measurements can be used as a sensitive test of the standard model not relying on precise atomic theory [13,14]. Proposals have been made for the measurement of atomic PNC in several isotopes of the one-valence electron systems of Ba$^+$ [15], and Fr and Ra$^+$ (produced at accelerator facilities such as TRIUMF [16] and KVI [17]) for which E^{PNC}_1 is expected to be enhanced compared to Cs [16,17], and theoretical precision expected to be better than 1%.

Here, we propose the measurement of PNC optical rotation in transitions of metastable Xe and Hg using a novel cavity-enhanced technique, having three main advantages: theoretical uncertainty for these two-electron excited states is expected to be better than all other systems mentioned except the alkalis; both Xe and Hg have large distributions of stable isotopes ($\Delta N/N = 12/76$ and $8/120$, respectively); and the proposed PNC measurements will be performed in a tabletop experiment. These three advantages should motivate all-order atomic-structure calculations for Hg and Xe, to investigate isotope and nuclear-spin-dependent effects, and whether sub-1% theoretical precision is possible.

PNC optical rotation φ_{PNC} is caused by the interference of a magnetic dipole ($M1$) transition and a PNC-induced electric dipole (E^{PNC}_1) transition, given by [6]

$$\varphi_{PNC} = -\frac{4\pi l}{\lambda}(n(\omega) - 1)\mathcal{R}, \qquad (1)$$

where $\mathcal{R} \equiv \mathrm{Im}(E^{PNC}_1)/M1$, l is the length of vapor, λ is the optical wavelength, ω is the optical frequency, and $n(\omega)$ is the refractive index due to the absorption line.

We identify the following favorable PNC transitions in metastable Xe, $(^2P^o_{3/2})6s\,^2[3/2]^o_2 \rightarrow (^2P^o_{1/2})6s\,^2[1/2]^o_1$ at 988 nm, and in Hg, $6s6p\,^3P^o_J \rightarrow 6s6p\,^1P^o_1$ at 609 nm ($J = 0$), 682 nm ($J = 1$), and 997 nm ($J = 2$). These first calculations of $\mathcal{R}$, for Xe and Hg, use the particle-hole approach described in Ref. [18]. We use the notation that $|hp\rangle$ describes an excitation of the ground state where an electron in state h forms a hole when it is excited to a state p. When a PNC enhancement factor arises from the presence of an opposite parity state n, nearly degenerate with the final state f in the transition $i \rightarrow f$, the PNC matrix element can be approximated by [13,14]

$$E_1^{\mathrm{PNC}} = \frac{1}{\Delta E} \langle f|H_{\mathrm{PNC}}|n\rangle\langle n|D|i\rangle, \qquad (2)$$

where ΔE is given in Fig. 1, D is the dipole operator, and appropriate sums over the angular momentum of n are understood. We introduce mixing coefficients n_i, and write $|n\rangle = n_1|5p_{1/2}6p_{3/2}\rangle + n_2|5p_{1/2}6p_{1/2}\rangle + n_3|5p_{3/2}6p_{3/2}\rangle + n_4|5p_{3/2}6p_{1/2}\rangle$. Because H_{PNC} mixes only s and $p_{1/2}$ states, only these components (with coefficients n_2 and n_4) give nonzero matrix elements when $\langle f|H_{\mathrm{PNC}}|n\rangle$ is evaluated. If the final state is written as $|f\rangle = f_1|5p_{3/2}6s\rangle + f_2|5p_{1/2}6s\rangle$, the matrix element of H_{PNC} reduces to the one-body operator $(n_2 f_2 + n_4 f_1) \times \langle 6s|H_{\mathrm{PNC}}|6p_{1/2}\rangle$. Values of the mixing coefficients can be obtained from standard atomic codes, but the level of precision to which they can be calculated is an open question. For the present calculation we use $n_2 = 0.030$, $n_4 = 0.746$, $f_1 = 0.062$, and $f_2 = 0.998$. For these values, $M1 = 0.0042ea_0$ and $\mathcal{R} = 11(3) \times 10^{-8}$, where the large uncertainty is caused by the difficulty in evaluating the small mixing terms that occur in H_{PNC}.

For Hg the situation is somewhat simpler, as $|n\rangle = |6s7s\rangle$, though we still need accurate values of f_1 and f_2 in $|f\rangle = f_1|6s6p_{1/2}\rangle + f_2|6s6p_{3/2}\rangle$. In this case we use $f_1 = 0.507$ and $f_2 = 0.862$ and find, for $J = 0$, 1, and 2, $\mathcal{R} = 14(3)$, 5(1), and $10(2) \times 10^{-8}$, and $M1 = 0.0014$, 0.0042, and $0.0057ea_0$, respectively. Note that $\mathcal{R}$ for Xe and Hg are similar, as the Xe E_1^{PNC} enhancement from the small ΔE denominator is largely canceled by the small value of n_2; also these $\mathcal{R}$ values are comparable to those of Tl, Bi, and Pb for which $\mathcal{R}$ is 15, 10, and 10×10^{-8} respectively [4–6]. The estimated error is based on the behavior of low order MBPT calculations. An accurate experimental measurement of PNC in either atom should stimulate theoretical work on a scale comparable to that carried out on Cs.
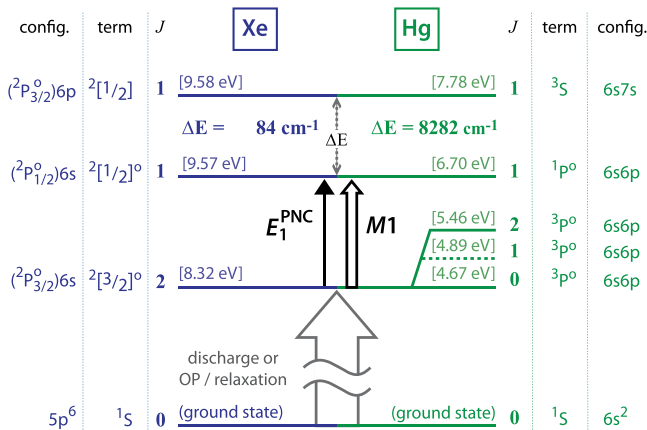
To obtain measurable PNC optical rotation signals, column densities of $\sim 10^{18}$ cm^{-2} thermal atoms are typically required [4–6], so as to achieve about 20 absorption lengths, for which optical rotation is $\sim 5\mathcal{R}$. Such column densities of excited-state atoms are generally not available due to the short excited-state lifetimes. The metastable states Xe $^3P_2$ and Hg ^3P_J have been produced at steady-state densities of about 10^{12} cm^{-3}, using electrical discharge lamps [19,20] or optical pumping [21], allowing column densities of about 10^{14} cm^{-2} (over a path length of 100 cm). For these column densities and calculated values of $\mathcal{R}$, an enhancement factor of about 10^4 is necessary to obtain signal levels comparable to previous optical rotation experiments [4–6].

Optical cavities have been used to enhance linear-birefringence by more than 10^4, using either polarimetric techniques or frequency metrology, in searches for magnetically-induced birefringence of vacuum [22], characterization of mirror birefringence [23,24], and measurements of the Cotton-Mouton [25,26] and Kerr effects in gases [27,28] with a sensitivity of 3×10^{-13} rad [28]. Linear optical cavities have been used for the enhancement of circular birefringence, such as for the Faraday effect of gases [29], and the optical activity of chiral molecules with the use of intracavity quarter-wave plates [30,31].

We propose the use of a four-mirror bow-tie cavity with counterpropagating laser beams for the enhancement of PNC measurements, outlined in Fig. 2. For a single pass in the cavity, the light polarization undergoes PNC rotation φ_{PNC} and Faraday rotation θ_F (produced by an applied longitudinal magnetic field). The different symmetry of these rotations under time reversal results in $\varphi_{\mathrm{PNC}} \rightarrow \varphi_{\mathrm{PNC}}$ and $\theta_F \rightarrow -\theta_F$ in the light-propagation frame (and $\varphi_{\mathrm{PNC}} \rightarrow -\varphi_{\mathrm{PNC}}$ and $\theta_F \rightarrow \theta_F$ in the lab frame), causing a difference in rotation for the clockwise (CW) and counter-clockwise (CCW) counterpropagating beams: $\alpha_{\mathrm{CW}} = \theta_F + \varphi_{\mathrm{PNC}}$ and $\alpha_{\mathrm{CCW}} = -\theta_F + \varphi_{\mathrm{PNC}}$. This directional symmetry breaking is key for the sensitive measurement of PNC optical rotation, in close analogy to Sagnac interferometry [32].

The Faraday effect splits the cavity spectrum into R and L circular polarization modes by $2\omega_F$, whereas the PNC rotation splits the CW and CCW modes by $2\omega_{\mathrm{PNC}}$, resulting in the cavity modes R_{CW}, L_{CW}, R_{CCW} and L_{CCW} [Fig. 2(b)]. The ratio of these splittings yields $\mathcal{R}$:

$$\mathcal{R} \equiv \frac{\mathrm{Im}(E_1^{\mathrm{PNC}})}{M1} = \frac{\omega_{\mathrm{PNC}}}{\omega_F} D(\omega)B, \qquad (3)$$

where $D(\omega) = (4\pi h/\mu_B)[(n(\omega) - 1)/(\partial n/\partial\omega)]$ is a line-shape-dependent factor [33], B is the longitudinal magnetic field, $\omega_{\mathrm{PNC}} = \varphi_{\mathrm{PNC}}c/L$, and $\omega_F = \theta_F c/L$ (where L is the cavity round-trip length).

To measure φ_{PNC}, a linearly polarized laser beam is split into two beams of equal intensity: one beam excites the R_{CW} mode (the reflected part of which is used for locking

FIG. 1 (color online). Partial energy level diagram of Xe and Hg (not to scale) showing the proposed E_1^{PNC} and $M1$ transitions.
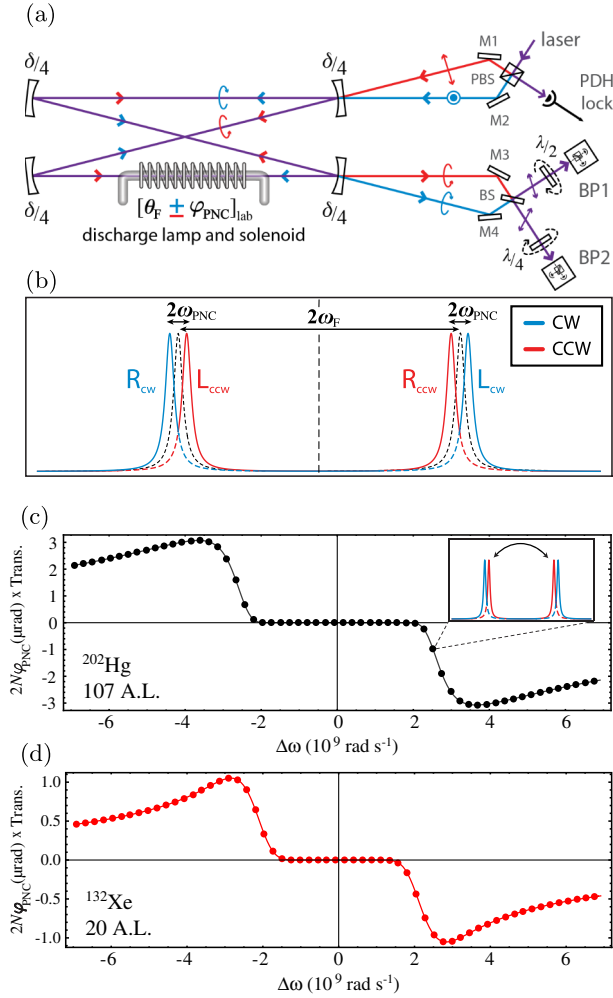
FIG. 2 (color online).   (a) Proposed experimental setup. (b) The
laser beam is frequency shifted with an AOM to be on resonance
with the nearly degenerate R_{CW}-L_{CCW} modes of the cavity. The
magnetic field splits the eigenmodes by $2\omega_F = 2\theta_F c/L$, while
ω_{PNC} (not to scale) is much smaller than the cavity linewidth. The
counterpropagating outputs are recombined into linearly polarized
light, and analyzed with linear and circular balanced polarimeters
(BP1 and BP2, respectively, using rotating half-wave and quarter-
wave plates). (c) Theoretical prediction of PNC optical rotation
signal $(2N\varphi_{PNC}(\mu rad) \times transmission)$ measured by BP1 and
BP2, corresponding to 107 absorption lengths (A.L.) of isotopi-
cally pure metastable ^{202}Hg. Alternating between the polarization
mode pairs (split by ~0.1 MHz), shown in the inset, yields a net
polarization difference $2N\varphi_{PNC}$, occurring at each black point,
which are separated by one FSR ($2\pi \times 37.5$ MHz). (d) similar to
(c), but for 20 A.L. of metastable ^{132}Xe (see text).

the laser frequency to the R_{CW} mode using the Pound-
Drever-Hall (PDH) scheme [34]) while the other beam
excites the nearly degenerate L_{CCW} mode (possible be-
cause ω_{PNC} is much smaller than the cavity linewidth
~1 kHz). The R_{CW} and L_{CCW} output beams are spatially
recombined to produce a linearly polarized beam rotated
by $N\varphi_{PNC}$, where N is the average number of round-trip
cavity passes. Our detection system measures the complete

set of the Stokes parameters of the output light [35], and
therefore directly determines φ_{PNC} and any experimental
depolarization effects.

A key point of the experiment is the availability of two
rapid experimental reversals: reversing either the magnetic
field direction or alternating the frequency of the CW and
CCW beams into resonance with the R_{CW}-L_{CCW} and
R_{CCW}-L_{CW} mode pairs. These reversals give a signal out-
put of $-N\varphi_{PNC}$ and a net difference in polarization rota-
tion of $2N\varphi_{PNC}$. The magnetic field and mode-pair
reversals can be performed quickly (up to 100 Hz) to
subtract slow experimental drifts. Measurement of the
difference in mode-pair frequencies gives $2\omega_F$ (see Fig. 2).

Theoretical calculations for the expected PNC rotation
signals are presented in Figs. 2(c) and 2(d). We assume a
four-mirror bow-tie cavity of round-trip cavity length $L =$
8 m (free spectral range, FSR = 37.5 MHz), mirror reflec-
tivity $R = 99.99\%$ (enhancement factor $N \sim 10^4$), and a
discharge lamp of length $l = 1.3$ m operating with isotopi-
cally pure ^{202}Hg (at 400 K) and ^{132}Xe (at 300 K). We note
that all even isotopes will have similar spectra, whereas
odd isotopes will have hyperfine structure; in addition, all
eight Xe and seven Hg stable isotopes are commercially
available (each low pressure lamp requires ~1 μmol of
isotopically pure gas). We plot the PNC optical rotation,
$2N\varphi_{PNC}$, multiplied by the transmission, as a function of
the laser frequency about the absorption line center, for
metastable ^{202}Hg column densities of 3.8×10^{18} cm^{-2}
(~ 107 absorption lengths) [19], and ^{132}Xe column den-
sities of 1×10^{18} cm^{-2} (~ 20 absorption lengths) [20].
Collisional line broadenings for Hg and Xe are estimated
to be 20 and 10 MHz, respectively. The black and red
points shown in Figs. 2(c) and 2(d) correspond to consecu-
tive longitudinal cavity modes separated by one FSR, so
that reasonable spectral resolution can be obtained even for
a fixed cavity.

We take advantage of the fact that a large applied
circular birefringence strongly suppresses effects of un-
wanted linear birefringences, which were important
sources of systematic errors in past PNC optical rotation
experiments, originating from mirror s-p phase shifts [36],
window transmission, and from stray transverse magnetic
fields [6,37]. A complete analysis of the polarization prop-
erties of the cavity, is performed using a Jones matrix
formulation [38]. For a four-mirror cavity with single
pass linear birefringence δ and circular birefringence α
the eigensystem is given by

$$\lambda_\pm = \cos\alpha \cos\frac{\delta}{2} \pm \sqrt{\cos^2\alpha\cos^2\frac{\delta}{2} - 1}, \qquad (4)$$

and

$$\nu_\pm = A\begin{pmatrix} \csc\alpha\left(\cos\alpha\sin\frac{\delta}{2} \pm \sqrt{1 - \cos^2\alpha\cos^2\frac{\delta}{2}}\right) \\ -i \end{pmatrix}, \qquad (5)$$
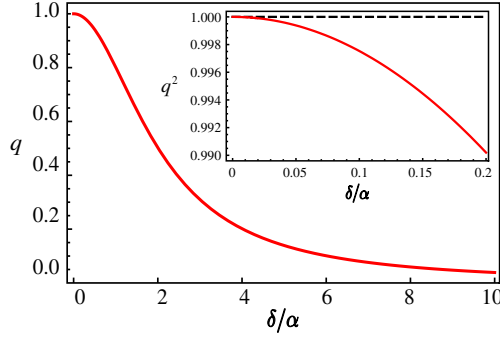
FIG. 3 (color online).   Numerical analysis of the dependence of the correction factors q and q^2 on δ/α.

FIG. 4 (color online).   Nonresonant Faraday effect of an intra-cavity SiO_2 window at 800 nm. The cavity ring-down polarization beating frequencies for counterpropagating beams are visibly different (magnetic field of 1000 G). The inset shows the linear and antisymmetric magnetic-field dependence of $\omega_{CW} - \omega_{CCW}$.

where A is a normalization constant. Here, for simplicity, we set the reflectivities for the s and p polarizations to be equal, which is a good approximation for near-normal angle-of-incidence bow-tie cavities. In the ideal case, where $\delta = 0$, the eigenvalues are equal to $\lambda_\pm = e^{\pm i\alpha}$ (with $\alpha_{CW} = \theta_F + \varphi_{PNC}$ and $\alpha_{CCW} = -\theta_F + \varphi_{PNC}$), which results in the four-mode spectrum described above and in Fig. 2(b).

For $\delta \neq 0$, the cavity eigenmodes are elliptical polarization states whose splitting is $\Gamma = \cos^{-1}[\cos\alpha \cos(\delta/2)]$. The noncommutative nature of linear and circular birefringence results in a reduction of the effective amplification of circular birefringence (Faraday and PNC rotation). We express the reduction effect as $\omega'_{PNC} = q\omega_{PNC}$, where $q = \alpha/\Gamma$ ranging from 1 to 0 (Fig. 3). Furthermore, with increasing δ the frequency-splitting of the polarization eigenmodes increases as $\omega'_F = (1/q)\omega_F$. Thus, δ reduces the observed ratio ω'_{PNC}/ω'_F by q^2:

$$\frac{\omega'_{PNC}}{\omega'_F} = pq^2 \frac{\omega_{PNC}}{\omega_F}, \tag{6}$$

where p is the degree of linear polarization of the output light which is reduced from 1 for unequal intensities or imperfect overlap of the recombining beams. We plot the correction factors q and q^2 in Fig. 3. Note that for $\delta \gg \alpha$ the circular birefringence (including PNC optical rotation) vanishes, a direct consequence of the transformation of the eigenpolarization modes into two linear polarization vectors. To ensure $q^2 \simeq 1$ we require $\delta \ll \alpha$. For example, for $q^2 \simeq 0.99$, $\delta = 0.2\alpha$, and for $q^2 \simeq 0.9999$, $\delta = 0.02\alpha$ (inset Fig. 3). For the $M1$ transitions and proposed conditions, the Faraday effect yields $\alpha \simeq 10^{-3}$ rad for a 200 G magnetic field [39], while mirror birefringence $\delta \lesssim 10^{-5}$ rad is achievable. Alternatively, antireflection (AR) coated windows with losses of $\lesssim 10^{-4}$ can be used to produce $\alpha \simeq 10^{-2}$ rad for a 1 T magnetic field and window birefringence $\delta \lesssim 10^{-4}$ rad.

To support the proposed experimental setup we demonstrate the mode structure of a bow-tie cavity using polarization-dependent cavity ring-down measurements [31] of the nonresonant Faraday effect of an intracavity
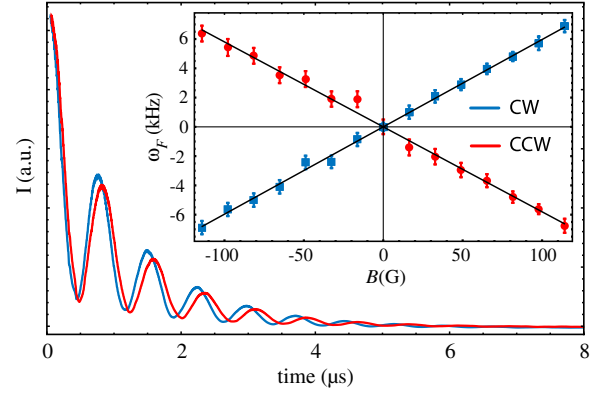
AR-coated SiO_2 window of 3 mm thickness. Two linearly-polarized pulsed beams ($\tau_{pulse} \simeq 35$ fs, $\lambda = 800$ nm, coherent bandwidth ~ 40 nm) are injected into counter-propagating modes of a four-mirror bow-tie cavity ($L = 3.7$ m). After exiting the cavity, the two beams enter separate balanced polarimeters [in contrast to Fig. 2(a)]. By making the cavity nonplanar, we introduce a purely geometric chiral rotation (of the same symmetry as PNC rotation) [40]. We adjust the rotation angle to be $\alpha_C = 2.9°$ per round-trip, resulting in a large mode splitting of $\omega_C = \alpha_C(c/L) = 4.15$ MHz (for the proposed PNC experiment ω_C must be minimized to be less than a cavity linewidth). The rotation of the polarization appears as a beating in the balanced polarimeters with frequency ω_C [31]. In the presense of Faraday rotation, the polarization beating of the two counterpropagating beams are different, $\omega_{CW} = \omega_F + \omega_C$ and $\omega_{CCW} = -\omega_F + \omega_C$, as shown in Fig. 4. We measure ω_{CW} and ω_{CCW} as a function of the magnetic field and show that their difference, $\omega_{CW} - \omega_{CCW} = 2\omega_F$, is linear with the magnetic field and changes sign upon magnetic-field reversal. The measured Verdet constant of SiO_2 at 800 nm is $(2.41 \pm 0.05)\ \mu rad\,G^{-1}\,cm^{-1}$, in agreement with [41].

Our cavity proposal can also be used for PNC optical rotation in other atoms [4–6,33,42], searches for permanent electric dipole moments (EDM) [43], and optical rotation or circular dichroism from chiral molecules [31].

*jsapirst@nd.edu
†ptr@iesl.forth.gr

[1] M. A. Bouchiat and C. Bouchiat, Phys. Lett. B **48**, 111 (1974).

[2] C. S. Wood, S. C. Bennett, D. Cho, B. P. Masterson, J. L. Roberts, C. E. Tanner, and C. E. Wieman, Science **275**, 1759 (1997).

[3] K. Tsigutkin, D. Dounas-Frazer, A. Family, J. E. Stalnaker, V. V. Yashchuk, and D. Budker, Phys. Rev. Lett. **103**, 071601 (2009).

[4] P. Vetter, D. M. Meekhof, P. K. Majumder, S. K. Lamoreaux, and E. N. Fortson, Phys. Rev. Lett. **74**, 2658 (1995).

[5] M. D. Macpherson, K. P. Zetie, R. B. Warrington, D. N. Stacey, and J. P. Hoare, Phys. Rev. Lett. **67**, 2784 (1991).

[6] D. M. Meekhof, P. Vetter, P. K. Majumder, S. K. Lamoreaux, and E. N. Fortson, Phys. Rev. Lett. **71**, 3442 (1993).

[7] L. M. Barkov and M. Zolotorev, Zh. Eksp. Teor. Fiz. **79**, 713 (1980) [Sov. Phys. JETP **52**, 360 (1984)].

[8] G. N. Birich, Y. V. Bogdanov, S. I. Kanorskii, I. I. Sobel'man, V. N. Sorokin, I. I. Struk, and E. A. Yukov, Zh. Eksp. Teor. Fiz. **87**, 776 (1984) [Sov. Phys. JETP **60**, 442 (1984)].

[9] V. A. Dzuba, V. V. Flambaum, and J. S. M. Ginges, Phys. Rev. D **66**, 070613 (2002).

[10] S. A. Blundell, W. R. Johnson, and J. Sapirstein, Phys. Rev. Lett. **65**, 1411 (1990).

[11] S. G. Porsev, K. Beloy, and A. Derevianko, Phys. Rev. D **82**, 036008 (2010).

[12] P. G. Kozlov, S. G. Porsev, and W. R. Johnson, Phys. Rev. A **64**, 052107 (2001).

[13] V. A. Dzuba and V. V. Flambaum, Phys. Rev. A **83**, 042514 (2011).

[14] D. DeMille, Phys. Rev. Lett. **74**, 4165 (1995).

[15] N. Fortson, Phys. Rev. Lett. **70**, 2383 (1993).

[16] E. Gomez, L. A. Orozco, and G. D. Sprouse, Rep. Prog. Phys. **69**, 79 (2006).

[17] L. W. Wansbeek, B. K. Sahoo, R. G. E. Timmermans, and K. Jungmann, Phys. Rev. A **78**, 050501 (2008).

[18] E. Avgoustoglou, W. R. Johnson, D. R. Plante, J. Sapirstein, S. Sheinerman, and S. A. Blundell, Phys. Rev. A **46**, 5478 (1992).

[19] J. J. Curry, G. G. Lister, and J. E. Lawler, J. Phys. D **35**, 2945 (2002).

[20] R. Bussiahn, G. Gortchakov, H. Lange, and D. Uhrlandt, J. Appl. Phys. **95**, 4627 (2004).

[21] W. Happer, Rev. Mod. Phys. **44**, 169 (1972).

[22] F. Bielsa, R. Battesti, C. Robilliard, G. Bialolenker, G. Bailly, G. Trénec, A. Rizzo, and C. Rizzo, Eur. Phys. J. D **36**, 261 (2005).

[23] J. L. Hall, J. Ye, and L.-S. Ma, Phys. Rev. A **62**, 013815 (2000).

[24] G. Bailly, R. Thon, and C. Robilliard, Rev. Sci. Instrum. **81**, 033105 (2010).

[25] D. Chauvat, A. L. Floch, M. Vallet, and F. Bretenaker, Appl. Phys. Lett. **73**, 1032 (1998).

[26] M. Bregant, G. Cantator, S. Carusotto, R. Cimino, F. D. Valle, G. D. Domenico, U. Gastaldi, M. Karuza, V. Lozza, and E. Milotti *et al.*, Chem. Phys. Lett. **471**, 322 (2009).

[27] E. Inbar and A. Arie, Appl. Phys. B **70**, 849 (2000).

[28] M. Durand, J. Morville, and D. Romanini, Phys. Rev. A **82**, 031803 (2010).

[29] M. Vallet, F. Bretenaker, A. L. Floch, R. L. Naour, and M. Oger, Opt. Commun. **168**, 423 (1999).

[30] J. Poirson, M. Vallet, F. Bretenaker, A. L. Floch, and J. Thepot, Anal. Chem. **70**, 4636 (1998).

[31] T. Muller, K. Wiberg, P. Vaccaro, J. Cheeseman, and M. J. Frischand, J. Opt. Soc. Am. B **19**, 125 (2002).

[32] W. W. Chow, J. Gea-Banacloche, L. M. Pedrotti, V. E. Sanders, W. Schleich, and M. O. Scully, Rev. Mod. Phys. **57**, 61 (1985).

[33] D. F. Kimball, Phys. Rev. A **63**, 052113 (2001).

[34] R. W. P. Drever, J. L. Hall, F. V. Kowalski, J. Hough, G. M. Ford, A. J. Munley, and H. Ward, Appl. Phys. B **31**, 97 (1983).

[35] H. G. Berry, G. Gabrielse, and A. E. Livingston, Appl. Opt. **16**, 3200 (1977).

[36] M. A. Bouchiat and L. Pottier, Appl. Phys. B **29**, 43 (1982).

[37] J. D. Taylor, P. E. G. Baird, R. G. Hunt, M. J. D. Macpherson, G. Nowicki, P. G. H. Sandars, and D. N. Stacey, J. Phys. B **20**, 5423 (1987).

[38] W. M. Doyle and M. B. White, J. Opt. Soc. Am. **55**, 1221 (1965).

[39] G. J. Roberts, P. E. G. Baird, M. W. S. M. Brimicombe, P. G. H. Sandars, D. R. Selby, and D. N. Stacey, J. Phys. B **13**, 1389 (1980).

[40] A. C. Nilsson, E. K. Gustafson, and R. L. Byer, IEEE J. Quantum Electron. **25**, 767 (1989).

[41] C. Tan and J. Arndt, J. Phys. Chem. Solids **60**, 1689 (1999).

[42] D. V. Neuffer and E. D. Commins, Phys. Rev. A **16**, 844 (1977).

[43] D. Budker, W. Gawlik, D. F. Kimball, S. M. Rochester, V. V. Yashchuk, and A. Weis, Rev. Mod. Phys. **74**, 1153 (2002).